AD_____

Award Number: W81XWH-05-2-0025

TITLE: Evaluation of Purine Salvage as a Chemotherapeutic Target in the Plasmodium yoelii Rodent Model

PRINCIPAL INVESTIGATOR: Kami Kim, M.D.

CONTRACTING ORGANIZATION: Albert Einstein College of Medicine
Bronx, NY 10461 USA

REPORT DATE: March 2008

TYPE OF REPORT: Annual

PREPARED FOR: U.S. Army Medical Research and Materiel Command
Fort Detrick, Maryland 21702-5012

REPORT DOCUMENTATION PAGE

Form Approved
OMB No. 0704-0188

1. REPORT DATE *(DD-MM-YYYY)*	**2. REPORT TYPE**	**3. DATES COVERED** *(From - To)*
01-03-2008	Annual	1 FEB 2007 - 31 JAN 2008

4. TITLE AND SUBTITLE

Evaluation of Purine Salvage as a Chemotherapeutic Target in the Plasmodium yoelii Rodent Model

5a. CONTRACT NUMBER

5b. GRANT NUMBER
W81XWH-05-2-0025

5c. PROGRAM ELEMENT NUMBER

6. AUTHOR(S)
Kami Kim, MD.

E-Mail: kkim@aecom.yu.edu

.5d. PROJECT NUMBER

5e. TASK NUMBER

5f. WORK UNIT NUMBER

7. PERFORMING ORGANIZATION NAME(S) AND ADDRESS(ES)

Albert Einstein College of Medicine
Bronx, NY 10461 USA

8. PERFORMING ORGANIZATION REPORT NUMBER

9. SPONSORING / MONITORING AGENCY NAME(S) AND ADDRESS(ES)
U.S. Army Medical Research and Materiel Command
Fort Detrick, Maryland 21702-5012

10. SPONSOR/MONITOR'S ACRONYM(S)

11. SPONSOR/MONITOR'S REPORT NUMBER(S)

12. DISTRIBUTION / AVAILABILITY STATEMENT
Approved for Public Release; Distribution Unlimited

13. SUPPLEMENTARY NOTES

14. ABSTRACT
Because resistance to current antimalarials is widespread, new targets for malaria chemotherapy are needed to protect military personnel stationed in developing countries. Malaria parasites cannot make purines needed for RNA and DNA and must salvage purines from their host. We are investigating whether the malaria purine salvage pathway can be exploited to develop specific treatments for malaria that will be effective but not toxic. We perform our studies in Plasmodium yoelii, a rodent malaria. We have genetically disrupted purine salvage enzyme purine nucleoside phosphorylase (PNP) and have shown that these P.yoelii parasites are attenuated and confer protective immunity to subsequent lethal challenge. We have also mapped residues in PNP responsible for the unique methylthiopurine activity. New protocols for transfection have been developed and we now have succeeded in attempts to disrupt adenosine deaminase (ADA). Both PNP and ADA deficient parasites are unable to form oocysts in the mosquito. We have developed GFP and GFP-luciferase reporter P. yoelii parasite lines that are able to complete the entire life cycle in mosquito and rodent hosts. The GFP-luciferase reporter parasites can be visualized in vivo by detection of bioluminescence both during intrahepatic and erythrocytic development. Initial studies suggest that we can use these parasites to test efficacy of drugs against exoerythrocytic malaria forms. We hope these experiments will lead to the development of new effective and nontoxic agents that can protect our military personnel from the lethal effects of malaria infection.

15. SUBJECT TERMS
Malaria, chemotherapy, purine, transfection

16. SECURITY CLASSIFICATION OF:			**17. LIMITATION OF ABSTRACT**	**18. NUMBER OF PAGES**	**19a. NAME OF RESPONSIBLE PERSON**
					USAMRMC
a. REPORT	**b. ABSTRACT**	**c. THIS PAGE**			**19b. TELEPHONE NUMBER** *(include area code)*
U	U	U	UU	35	

Standard Form 298 (Rev. 8-98)
Prescribed by ANSI Std. Z39.18

Table of Contents

Evaluation of Purine Salvage as a Chemotherapeutic Target in the *Plasmodium yoelii* Rodent Model
W81XWH-05-2-0025
Kami Kim, MD

Introduction:

Because resistance to current antimalarials is widespread, new targets for malaria chemotherapy are needed to protect military personnel stationed in developing countries. Malaria parasites cannot make purines needed for RNA and DNA and must salvage purines from their host. Our preliminary studies reveal purine salvage is unique in malaria parasites. We would like to determine whether the unique activities of the malaria enzymes can be exploited to develop specific treatments for malaria that will be effective but not toxic. While study of drug targets in vivo is critical for all infectious diseases, evaluation in an animal model is especially critical for evaluation of purine salvage as a drug target. Malaria parasites are routinely maintained in the laboratory with high concentrations of purines, but levels of purines in mammalian blood are tightly regulated and 100-fold less than typical culture conditions. Therefore the efficacy of purine salvage inhibition and importance of purine salvage enzymes must be examined under physiological conditions that cannot be replicated during in vitro culture conditions. We plan to perform our studies in *Plasmodium yoelii*, a rodent malaria whose genome has been sequenced and for which there are techniques for genetic manipulation. Using this system we will genetically disrupt purine salvage genes and test their importance to the parasite. We will test the effects of malaria-specific purine salvage inhibitors on malaria infection in mice. These novel drugs will be tested in combination with other antimalarials and will also be evaluated for efficacy against exoerythrocytic malaria forms. We hope these experiments will lead to the development of new effective and nontoxic agents that can protect our military personnel from the lethal effects of malaria infection.

Task 1 PNP gene disruption in Plasmodium yoelii.

1. Make double cross-over constructs for PyPNP including one that replaces P. falciparum PNP for PyPNP. Months 1-3, year 1
2. Transfect, select and clone disruptants in mice. Months 4-12 year 1.
3. Analyze phenotype of disruptants and PfPNP replacements for mouse virulence, ability to complete the full life cycle, ability to transport and incorporate purines. Year 1 and year 2.

We have completed most of this task. Our manuscript describing our findings with the *Δpypnp* parasites is now in revision. As discussed in our revised progress report for 2007, these parasites are attenuated in blood stages and unable to make oocysts in mosquitoes. Mice administered the attenuated parasites are protected from subsequent lethal challenge. See figure 1 below, from our prior progress report. We are further investigating the virulence of these attenuated *Δpypnp* parasites in immunocompromised mice. It is possible that these parasites can be used for development as asexual stage attenuated vaccines similar to the attenuated sporozoites proposed by others.

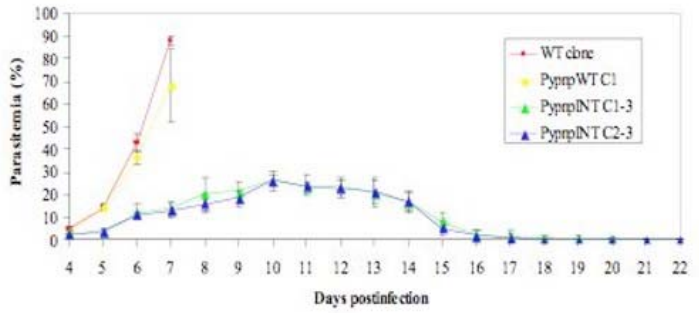

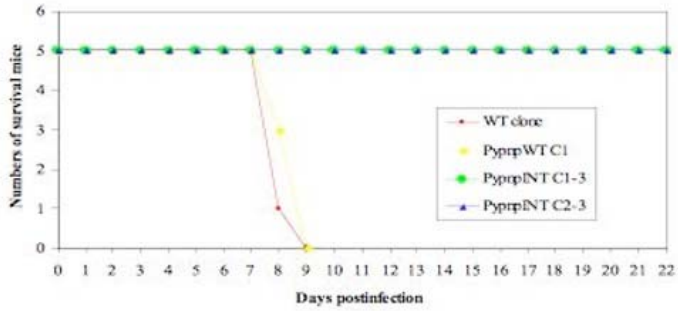

Figure 1: Parasitemias and survival of mice infected with wild-type, PNP disruptant (PypnpINT) or integrant with intact PNP (PypnpWT).

After the fate of the submitted manuscript is decided we will write a methods paper delineating our improved protocols for genetic manipulation of *Plasmodium yoelii* parasites. We have used this methodology for other studies in *P. yoelii* and a manuscript on disruption of *Pyhmgb2* has been accepted to JBC. Dr. Ting, lead personnel on this grant, assisted in the early studies for this manuscript.

Task 2 ADA disruption in *Plasmodium yoelii.*

1. Make single and double cross-over disruption constructs. Months 10-12, year 1
2. Transfect, select and clone disruptants. Months 1-6, year 2.
3. Analyze phenotype of disruptants for mouse virulence, ability to complete the full life cycle, ability to transport and incorporate purines. Months 7-12 year 2. Continue year 3

We have nearly completed this aim. After our successful development of double crossover gene deletion methodology for disruption of *Pypnp* (see aim 1), we were able to quickly delete the *PyADA* gene. Surprisingly, in contrast to *Δpypnp* parasites, *Δpyada* parasites are not significantly attenuated. We are repeating studies to have statistically robust numbers, but *Δpyada* parasites do have a profound defect in oocyst development. Although there was a significant delay in implementing this aim, we are now on target to complete this aim by the end of the funding period.

Task 3 Test the effect of immucillins on the P. yoelii rodent malaria model.

1. Test whether the immucillins with best in vitro activity or best malaria-specific activity can cure mice with malaria. Year 1-2
2. Test whether effective immucillins are effective against transgenic *P. yoelii* that carry PfPNP. Year 3
3. Compare effects of malaria specific immucillins to immucillins that inhibit only mouse PNP or inhibit both PNPs in wild-type and parasites with disruption in purine salvage genes. Year 3

Earlier in our funding period, we tested Immucillin-H, DADMe Immucillin-H, MT-Immucillin-H, and MT-coformycin against *P. yoelii* and *P.berghei.* Each of these inhibitors are able to kill cultured *P. falciparum* (Ting *et al,* and Madrid, Ting & Kim, unpublished). Unfortunately, none are able to cure mice. MT-ImmH, an inhibitor with 112-fold specificity for *P. falciparum* PNP, gave the best results with delay to death in some experiments. MT-coformycin is >20,000 more specific for PfADA over human ADA but was not efficacious although it has activity on cultured *P. falciparum* (Madrid, Ting and Kim, unpublished).

In related studies completed by our group (but not funded by this grant), we have disrupted *Pfpnp* and shown this renders *Δpfpnp* parasites less sensitive to MT-ImmH and much more sensitive to human PNP inhibitors. The *Δpfpnp* parasites, like *Δpypnp* parasites, are viable but attenuated at physiological concentrations of purines. Thus we have validated PNP as the major target of immucillins.

Because of these studies, we questioned whether the rodent malaria enzymes were as sensitive to the inhibitors as their *P. falciparum* orthologues. Therefore we cloned and fully characterized the rodent malaria PyPNP and PyADA (See alignments provided in 2007 progress report). Recombinant PyPNP was compared to PfPNP and its enzyme kinetics and inhibition profile are identical to that of PfPNP. Thus the inability of immucillins to cure mice infected with *P. yoelii* is not likely due to differences in the target PNP enzymes.

3Mut has reduced MTI activity

Enzyme 1μg/mL	Inosine k_{CAT}/K_M ($M^{-1}s^{-1}$)	5'MTI k_{CAT}/K_M ($M^{-1}s^{-1}$)	
PfPNP	$1.56x10^5$	$9.56x10^4$	
TgPNP	$2.41x10^5$	ND	
Pf Y160F	$2.2x10^5$	$1.48x10^4$	
PfPNP V66I/Y160F	$1.32x10^5$	$7.17x10^3$	
PfPNP V66I/V73I/ Y 160F	$1.82x10^5$	$3.94x10^2$	⇐biologically irrelevant

ND= Not detectable

Now that we have resolved some of the technical difficulties, we are finishing the constructs to replace PyPNP with PfPNP (#2 in this task). We have now mapped the key residues responsible for the methylthiospecificity of PfPNP by taking advantage of the finding that TgPNP is homologous to PfPNP but does not have activity against methylthiopurines (Chaudhary *et al*). We were able to determine that mutations in 3 key residues: V66I, V73I, Y160F were needed loss of MTI activity. The level of activity against MTI is 3 orders of magnitude less than wild-type and not biologically relevant.

We have also obtained the crystal structure of the triple mutant PfPNP with ImmH. This structure is now being refined and compared to the structure obtained earlier for PfPNP (Shi *et al*). The key findings to date reveal that 3Mut PfPNP has a more crowded pocket than WT PfPNP. While individually the Val66Ile and the Val73Ile have minimal effects, together they cause crowding of the pocket makes the methylthio group unable to fit easily. The OH group of the Tyr 160 stabilizes the hydrophobic pocket by hydrogen bonding with water molecules. Pocket residue placement is more flexible without the hydroxyl group due to Tyr160Phe mutation, further constraining the MTI pocket. We hope to compare this crystal to one in which 3Mut PfPNP is crystallized with MT-ImmH.

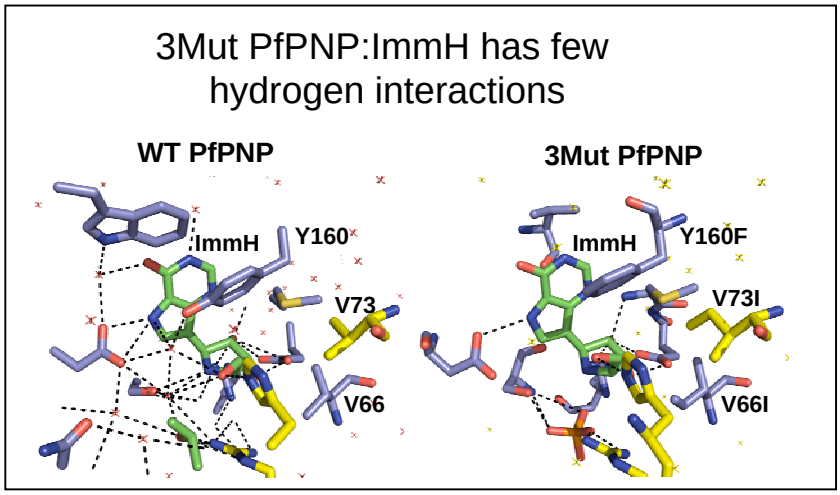

We will replace PyPNP with PfPNP with wild-type enzyme as well as with the triple mutant only activity against inosine to test the importance of the unique methylthiopurine substrate specificity for viability of *Plasmodium* parasites. Viability will be compared to parasites lacking *pypnp*. If the purine recycling activity of PNP is critical, the PNP mutant with activity against only inosine will be attenuated compared with the PfPNP wild-type transfectant.

Task 4 Test immucillins in combination with antimalarials

1. Establish dose response of agents (DFMO, deoxycoformycin, atovoquone, mycophenolic acid) against *P. yoelii.* Years 2-3
2. Test additive and synergistic effects of agents (particularly polyamine and ADA inhibitors) with best immucillin(s). Year 3-4
3. Test best drug combination for "causal" prophylaxis and cure after sporozoite challenge using *P. yoelii* sporozoites. Year 4

Dose response studies for agents to be used in combination were initiated. Because the immucillins were not effective in the rodent models we shifted our focus to verifying that recombinant enzyme targets were susceptible (see above). Previous studies reveal that the immucillins are bioavailable in mice. It seems probable that there are differences in purine metabolism between mice and humans that may make the rodent model less optimal for use evaluating purine salvage enzymes as drug targets. Similarly for immucillins currently in human clinical trials, effects were less pronounced in rodents than humans. Our results validate the importance of PNP in rodent and human malaria and validate PNP as the target of immucillins. Studies in nonhuman primates are needed to fully test the efficacy of immucillins as antimalarials.

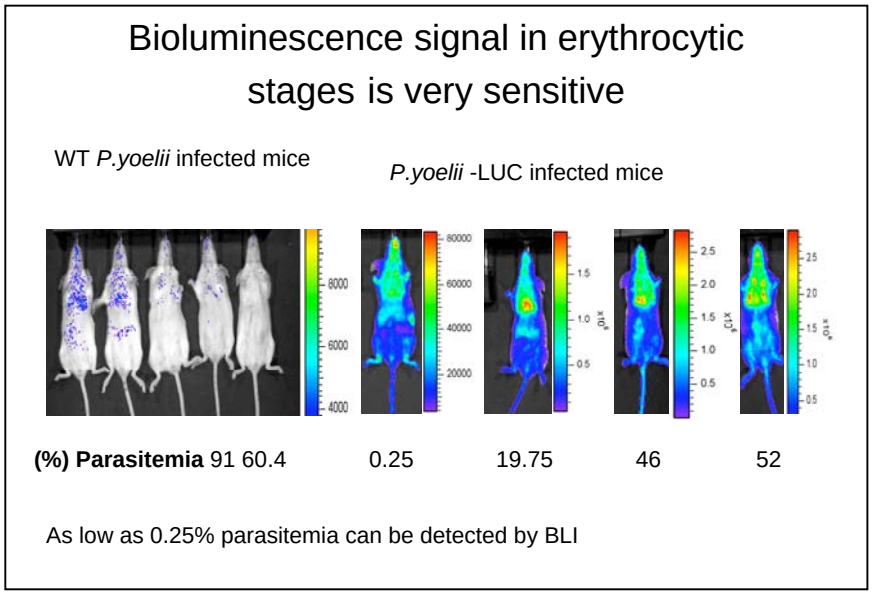

A major area that needs further investigation is the liver stages of malaria. Understanding and

targeting these stages has major impact upon military objectives to develop agents that target the liver stages as effective prophylactic agents. We have initiated a parallel effort to develop tools to better evaluate the efficacy of agents against the liver stages. We have been working on developing a reliable *in vitro* EEF development assay. The *in vitro* assays in hepatocytes were hampered by poor viability of the liver cells and poor development but we have now developed culturing protocols that reliably result in viable hepatocyte cultures.

In vivo studies with *P.yoelii* GFP/luc lines we have developed have been successful. These reporter parasites are readily detected by monitoring for bioluminescence even with low parasitemias (See figure above). Luciferase activity is proportional to parasitemias and can be detected in the liver at day 2 after infection (See figure below). We are completing pilot studies to test antimalarials against the liver stages. So far, as expected, atovoquone reduces liver luminescent signal but chloroquine is not effective against EEFs, but we are now repeating experiments to look at the reproducibility of our assays.

Liver exoerythrocytic forms of *P.yoelii*-LUC express luciferase

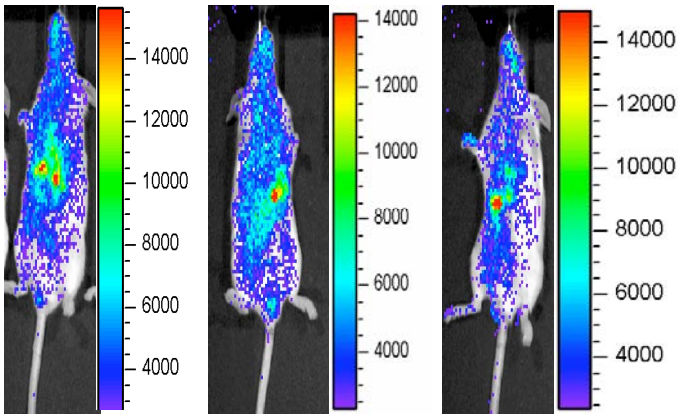

In vivo bioluminescence signal from livers of mice infected 2 days earlier with *P.yoelii - LUC*

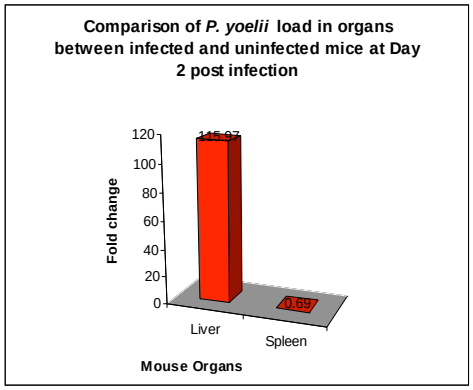

qPCR of *P.yoelii* 18s rRNA confirms the presence of EEFs in mice expressing bioluminescence.

Key Research Accomplishments:

1. Development of PCR-based methodology to rapidly knock-out genes by double homologous gene replacement in *P. yoelii* and application of this technique for disruption of *pypnp, pyada, pyhmgb2.*
2. Creation and validation of a GFP-luciferase reporter *P. yoelii* line able to complete the entire malaria life cycle in mice and mosquito hosts.

3. Illustration that Δ*pypnp* lines are attenuated and protective against subsequent lethal challenge.
4. Disruption of PyADA—full characterization ongoing.
5. Mapping residues in PfPNP for methylthio specificity.
6. Crystal structure of PfPNP lacking methythio specificity.
7. Visualization of hepatic and erythrocytic stages of *P. yoelii* using biolumenscence.

Reportable Outcomes:

Stable *P.yoelii* GFP-luciferase reporter parasite that can be used to monitor infection in mice by bioluminescence.

Manuscripts:

1. Gissot, M, LM Ting, T. Daly, LW Bergman, P Sinnis, **K Kim** High mobility group protein HMGB2 is a critical regulator of Plasmodium oocyst development Journal of Biological Chemistry 2008 In press.

Two other manuscripts have been submitted.

Conclusions:

Transfection studies are consistent with the hypothesis that PNP is important to viability of malaria parasites *in vivo*. Parasites lacking PyPNP are attenuated in blood stages, and have dramatically reduced development of oocysts. In addition, the attenuated blood stage parasites are protective against subsequent lethal challenge with *P. yoelii.* Attempts to disrupt ADA have finally been successful using a new technique for PCR mediated double homologous recombination, and preliminary studies suggest these parasites are unable to form oocysts. We have mapped the residues in PNP critical for methylthio activity and will genetically test the importance of the purine recycling activity of PNP. We have developed GFP-luciferase reporter parasites that are able to complete the entire life cycle and can be visualized during intrahepatic infection. These parasites are likely to be useful for development of *in vivo* and *in vitro* protocols for drug testing of antimalarials for erythrocytic and extraerythrocytic forms.

References:

Chaudhary K, Ting LM, Kim K, Roos DS. *Toxoplasma gondii* purine nucleoside phosphorylase biochemical characterization, inhibitor profiles, and comparison with the *Plasmodium falciparum* ortholog.J Biol Chem. 2006 Sep 1;281(35):25652-8. Epub 2006 Jul 7.
PMID: 16829527

Ecker A, Moon R, Sinden RE, Billker O. Generation of gene targeting constructs for *Plasmodium berghei* by a PCR-based method amenable to high throughput applications. Mol Biochem Parasitol. 2006 Feb;145(2):265-8. Epub 2005 Oct 24.
PMID: 16290088

Shi W, Ting LM, Kicska GA, Lewandowicz A, Tyler PC, Evans GB, Furneaux RH, Kim K, Almo SC, Schramm VL. *Plasmodium falciparum* purine nucleoside phosphorylase: crystal structures, immucillin inhibitors, and dual catalytic function. J Biol Chem. 2004 Apr 30;279(18):18103-6. Epub 2004 Feb 23.
PMID: 14982926

Ting LM, Shi W, Lewandowicz A, Singh V, Mwakingwe A, Birck MR, Ringia EA,Bench G, Madrid DC, Tyler PC, Evans GB, Furneaux RH, Schramm VL, Kim K. Targeting a novel *Plasmodium falciparum* purine recycling pathway with specific immucillins. J Biol Chem. 2005 Mar 11;280(10):9547-54. Epub 2004 Dec 2.
PMID: 15576366

JBC Papers in Press. Published on April 8, 2008 as Manuscript M801637200
The latest version is at http://www.jbc.org/cgi/doi/10.1074/jbc.M801637200

HIGH MOBILITY GROUP PROTEIN HMGB2 IS A CRITICAL REGULATOR OF *PLASMODIUM* OOCYST DEVELOPMENT

Mathieu Gissot[1], Li-Min Ting[1], Thomas M. Daly[2], Lawrence W. Bergman[2], Photini Sinnis[3] and Kami Kim[1*].

From [1]Departments of Medicine and of Microbiology & Immunology, Albert Einstein College of Medicine, Bronx, NY. [2]Department of Microbiology and Immunology, Drexel University College of Medicine, Philadelphia, PA. [3]Department of Medical Parasitology, New York University School of Medicine, New York, NY

Running Head: PyHMGB2 is a critical regulator of oocyst development

Address correspondence to: Kami Kim, Ullmann 1225, Albert Einstein College of Medicine, 1300 Morris Park Avenue, Bronx, NY 10461 USA. Ph: 01 718 430 2611; email: kkim@aecom.yu.edu

The sexual cycle of *Plasmodium* is required for transmission of malaria from mosquitoes to mammals, but how parasites induce the expression of genes required for the sexual stages is not known. We disrupted the *Plasmodium yoelii* gene encoding high mobility group nuclear factor *hmgb2*, which encodes a DNA binding protein potentially implicated in transcriptional regulation of malaria gene expression. We investigated its function *in vivo* in the vertebrate and invertebrate hosts. *Δpyhmgb2* parasites develop into gametocytes but have drastic impairment of oocyst formation. A global transcriptome analysis of the *Δpyhmgb2* parasites identified approximately 30 genes whose expression is downregulated in the *Δpyhmgb2* parasites. These genes are conserved in all malaria species and more than 90% of these genes show a peak of mRNA expression at the gametocyte stage. Surprisingly, the transcripts coding for the *P. berghei* orthologues of those genes are stored and translated in the ookinete stage. Therefore sexual stage protein expression appears to be both transcriptionally and translationally regulated with *Plasmodium* HMGB2 acting as an important regulator of malaria sexual stage gene expression.

Plasmodium species, the causative agents of malaria, are the most deadly members of the apicomplexan phylum. As with other members of the Apicomplexa, *Plasmodium* has a multifaceted life cycle encompassing an asexual phase within the intermediate host and a sexual cycle in the mosquito. Gametocytogenesis and gametogenesis consist of an ensemble of processes leading to the differentiation of erythrocytic forms of the parasite into male or female gametocytes. These complex and coordinated steps insure the transmission of the parasite to the invertebrate host and are required for transmission of malaria to mammalian hosts. Gametocytes form in mammalian host, are taken up by the mosquito during a blood meal, transform into gametes in the mosquito midgut and then fuse to form a zygote. Zygotes differentiate into ookinetes which penetrate the midgut wall and differentiate into oocysts, in which sporozoites will develop.

Starting from the well controlled vertebrate milieu, the parasite must adapt to the mosquito environment where temperature fluctuates and nutrients are limited. Gametocytogenesis requires growth arrest and a differentiation step that will prepare the parasite for these changes. Sexual differentiation is accompanied by a tightly controlled gene expression program during

which approximately 200-300 mRNAs are specifically expressed or predominantly expressed in sexual forms of the parasite (1-4). Transcriptional control of gene expression is implicated as a crucial step during this process with sex-specific transcript expression in gametocytes controlled by the sequences in the 5′ flanking regions (5).

For some sexual stage genes posttranslational processes mediate gene expression. The genes coding for P25 and P28 ookinete proteins (PY00522 and PY00523 respectively) are transcribed at the gametocyte stage but their translation is delayed until the gamete and zygote stages (6). A group of mRNAs with a common 3′UTR motif are specifically transcribed at the gametocyte stage but their translation is repressed until the parasite requires the presence of the proteins they encode (4). Recently an RNA helicase called DOZI (7) was identified in *P. berghei* that participates in the storage and translation repression of a large number of transcripts. Therefore, sexual differentiation in *Plasmodium* requires fine tuning of both transcriptional and post-transcriptional processes to regulate gene expression.

The mechanisms controlling the transition from the asexual erythrocytic stage into a gametocyte-specific gene expression program are unknown. Initial analysis of the genomes of *Plasmodium* species revealed few canonical transcriptional regulators (8). On the other hand, the RNA polymerase II machinery (9) is conserved within Apicomplexa and chromatin modification plays an important role in gene regulation (10). The finding that certain DNA motifs are recurrent in the promoters of Apicomplexa and bind to nuclear factors (11-13) suggests that unrecognized transcription factors exist. Recently, a novel family of AP2 domain plant-like transcription factors was identified in the genomes of the Apicomplexa (14). In plants these transcription factors bind to specific DNA motifs and regulate a variety of biological responses (15), but the function of apicomplexan AP2 proteins has not been experimentally validated.

Two proteins containing a high mobility group box (HMGB) are highly conserved among *Plasmodium* species (16). HMGB box proteins are small transcriptional regulators that bind DNA in a non-sequence specific fashion and bend it, leading to the recruitment of RNA polymerase II and the induction of transcription (17). HMGB proteins also actively participate in chromatin remodelling by increasing nucleosome sliding and accessibility of the chromatin (17). The two *P. falciparum* HMGB proteins, HMGB1 (PFL0145c) and HMGB2 (MAL8P1.72), have the biochemical characteristics of the HMGB box family of transcriptional regulators (16). Interestingly, these HMGB are differentially expressed. HMGB1 is expressed during the erythrocytic asexual cycle whereas HMGB2 is slightly expressed at the schizont stage and highly expressed at the gametocyte stage (2,16).

In this study, we evaluated the role of the HMGB2 protein in regulation of sexual stage gene expression. We disrupted *hmgb2* in the rodent malaria model *Plasmodium yoelii* and investigated its function *in vivo* in its two hosts: the mouse and the mosquito *Anopheles stephensi*. Our results indicate that PyHMGB2 plays a central and conserved role in regulating gene expression during the sexual cycle of *Plasmodium*.

Experimental Procedures

Plasmodium yoelii life cycle.

P. yoelii YM lethal strain was maintained in naïve BALB/c or Swiss Webster mice. For mosquito infection experiments 4–5-day-old *A. stephensi* were fed for 15 min on anesthetized Swiss Webster mice infected with either wild-type (WT) or *Δpyhmgb2 (*KO) *P. yoelii* parasites. Prior to feeding, the abundance and the sex ratio of the gametocyte-stage parasites was checked on Giemsa stained blood smears. At day 7 post-infection, midguts were monitored for infection and oocysts were counted by either counting fluorescent GFP-positive KO parasite oocysts (see below) or after mercurochrome staining (WT and KO parasite lines). Salivary glands from mosquitoes on day 14 or 15 post-infective blood meal (p.i.) were dissected to recover sporozoites.

Exflagellation experiments were performed as described in (18) and exflagellation centers were counted at 9 mins post induction. Male and female gametocytes were identified by morphology on Giemsa smears. *In vitro* culture of ookinetes was performed as described in (19). Ookinete numbers were counted with a hemacytometer under phase-contrast microscope and normalized to the original gametocyte content of the culture. Statistical analysis was performed using an un-paired *t*-test available using the GraphPad Prism software package (GraphPad software, San Diego, CA, USA).

P. yoelii transfection, plasmid construction and genotyping

A fragment of the *pyhmgb2* gene (PY07077) amplified from YM strain genomic DNA using the following primers (5'-ggatccATTACATGTTATGATCTTCTAC-3' and 5'-gcggccgc-CAATGCTCTCTTTGGAGCTAATG-3') was inserted into the pMD205-GFP vector in the *BamH1* and *NotI* restriction sites. A *SpeI* restriction site was created by site directed mutagenesis (Stratagene, La Jolla, CA, USA) at nucleotide position 258 of the cloned fragment (position 3152 of the MALPY02526 contig sequence) using the following primer (5'-TACAACTTTAGAACAAGACTAGTACTG TTTTGAAACAACTCA-3'). Prior to transfection, the targeting plasmid was linearized using a *SpeI* site created in the *pyhmgb2* open reading frame. Transfections were performed as described in (20,21). Cloning was performed after limiting dilution and infection of 20 BALB/c mice. A WT non recombinant clone was passaged in parallel with KO clones so that mouse and mosquito passage numbers were comparable for all experiments.

Diagnostic PCR was performed using the primers T7 (5'-TAATACGACTCACTATAGGG-3') and A (5'-ATCGATTAGTAGAATATGTAATATA-3') as indicated in Figure 1.

A probe containing a portion of the *pyhmgb2* gene was amplified by PCR and digoxigenin-labeled (DIG) using the DIG random prime labeling kit (Roche Applied Science, Indianapolis, IN, USA). Southern blot was performed after running 1 µg of *HindIII* digested genomic DNA on a 0.8 % agarose gel and passive transfer on a nylon membrane and revealed using an anti-DIG antibody coupled to peroxidase (Roche Applied Science, Indianapolis, IN, USA).

Infectivity and survival assays.

Five BALB/c or Swiss Webster mice per group were infected intravenously using $5x10^5$ and $1x10^6$ parasites respectively. Beginning twenty-four hours after injection a thin smear of blood was prepared daily and stained with Giemsa reagent. For each sample, at least 1000 RBCs were examined by microscopy, and the percentage of parasitized erythocytes was calculated. Mouse viability was monitored every 12 hours. Statistical analysis was performed using the GraphPad Prism software (GraphPad software, San Diego, CA, USA).

Microarray design and experiments

Two mice per group were infected with one million purified schizonts from the WT and two clones (B3 and D1) of the *Δpyhmgb2* lines. When parasitemia reached 10 to 20 % and equivalent gametocytemia, total RNA was extracted from the WT and the B3 and D1 clones of the KO parasite lines using the Trizol method on saponin lysed parasites. For each group, RNA originating from the two mice was pooled. Total RNA integrity was checked using the Agilent Bioanalyzer (Agilent Technologies, Santa Clara, CA, USA) at the AECOM shared sequencing facility.

P. yoelii microarrays were produced in the Molecular Genomics Core Facility, Drexel University College of Medicine under the direction of L.W.B. The spotted microarray contained 7,080 65mer oligonucleotides (probes). Each probe was spotted twice on the array. The array has been developed and previously evaluated with hybridizations of total RNA extracted from blood stages. Probe sequences were blasted against annotated *P. yoelii* genes downloaded

from PlasmoDB (version 5.2). In total, 6,451 probes were specifically mapped to 6,428 annotated *P. yoelii* genes with a perfect match (22).

To prepare each probe, 10 µg of *P. yoelii* RNA was reverse transcribed into cDNA in the presence of aminoallyl-dUTP (FairPlay microarray labeling kit; Stratagene, La Jolla, CA). The cDNA was then fluorescently labeled by reaction with monofunctional, normal *N*-hydroxysuccinimide-activated Cy3 or Cy5 dye (Amersham Biosciences Inc., Piscataway, NJ). The Cy dye-labeled cDNA was purified, and the yield and specific activity of each probe were determined by absorption spectroscopy. Pairs of Cy3- and Cy5-labeled probes were pooled and hybridized to the *P. yoelii* microarrays for 14 to 16 h at 60°C in a 60-µl mixture. Following hybridization and washing, slides were scanned using a GenePix 4000A microarray laser scanner (Axon Instruments Inc., Union City, CA), and the fluorescence intensity of each DNA feature was determined at 532 nm (Cy3) and at 635 nm (Cy5). Data for each gene were obtained from replicate features (n = 2). On a second set of arrays the assignments of Cy3 and Cy5 for labeling of the paired cDNA probes were reversed (standard dye flip). Gene expression data were acquired and analyzed using the GenePixPro 5.0 and Acuity 3.0 Microarray Informatics software (Axon Instruments). Two biological replicates with the proper dye swap controls were performed resulting in a total of 8 hybridization signals from each parasite line for each gene represented on the microarray. Data have been deposited to GEO database (GXXXX) together with the microarray platform (GPL5381).

Microarray normalization and statistical analysis

The .gpr files were loaded using the Bioconductor *limma* package. Quality assessment of the microarrays was performed using the package *arrayQuality*. The data was then normalized in order to remove systematic technical variation. Two-channel normalization was performed using the function maNorm in the package *marray*. Three types of normalization were performed: (i) using the median enabling global median location normalization; (ii) using a global normalization using the scatter-plot smoother loess; (iii) a 2 dimension spatial normalization using the loess function. Selection of differentially expressed genes was performed using the package *limma* that is based on the fitting of the expression data for each gene to a linear model. Empirical Bayes were then used to borrow information across genes making the analyses stable even for experiments with a small number of arrays (23). In this method, the basic statistic used for significance analysis is the moderated *t*-statistic. Moderated *t*-statistic lead to *p*-values with increased degrees of freedom reflecting the greater reliability associated with smoothed standards-errors (24). A *p*-value cut-off to 0.05 was set leading to a false discovery rate of 5 %.

RT-PCR and real time quantitative RT-PCR

One microgram of DNase treated total RNA was utilized to produce cDNA following the instructions of the first strand cDNA kit (Invitrogen) with oligo dT as a primer. PCR was performed during 30 cycles using the following primers: *pyada* forward (5'-ATGATGGAAATTCCAACTGAAGA-3'), *pyada* reverse (5'-TTAAAAGTACAACGCTTTAAGCTCG-3'), *pyhmgb2* forward (5'-CCTATCAAGTGTGTTGTATATGTCTTC-3') and *pyhmgb2* reverse (5'-TCTTCTATTTCTTTGGAATAACGAAC-3'). Real time quantitative PCR was performed on the 7300 ABI apparatus using the Power Sybr (Applied Biosystems, Foster City, CA) mastermix in a 20 µL volume according to the manufacturer's instructions. PCR primers were designed using the Primerexpress software (Applied Biosystems, Foster City, CA) to amplify regions of 100-150 nt. Each experiment was performed at least two times in duplicate. A list of other primers used for verification of microarray results by real-time quantitative RT-PCR is available in supplementary materials.

Western Blotting.

Ookinete cultures of WT and KO parasites containing a similar number of ookinetes (approximately $1x10^6$) were harvested by centrifugation and extracted with SDS-PAGE loading buffer. The extracts were size fractionated on SDS–12% polyacrylamide gels and proteins were transferred to polyvinylidene difluoride membrane . The membrane was incubated over-night at 4ºC with mouse monoclonal anti-Pys21 (also named Pys25) and anti-Pys25 (also named Pys28) antibodies (A gift from Dr. T. Tsuboi, Ehime University, Japan;(25)) diluted 1/500 and an anti-PyADA antibody diluted 1/1000 in a PBS-5% milk solution. The membrane was then incubated 1 hour at room temperature with a 1:10,000 dilution of peroxidase-conjugated anti-mouse antibody. After extensive washing, signal was revealed using a chemiluminescent substrate, according to the manufacturer's instructions (ECL, Amersham-Pharmacia Biotech). Relative amounts of proteins were determined by densitometry using the Quantiscan software (Densylab, Microvision Instruments, Evry, France). Relative expression of Pys25 and Pys28 in wild-type and KO was normalized by comparing the level of expression of the PyADA protein in each sample.

Results

Disruption of the pyhmgb2 *locus*

Disruption of the *pyhmgb2* locus was performed after integration of a plasmid containing a segment of the *pyhmgb2* gene and the selectable marker cassette PbDHFR-TS fused to the GFP gene. The integration of this plasmid at the *pyhmgb2* locus created two copies of the truncated gene after a single cross-over event (Fig.1A). Two independent *pyhmgb2* knock-out clones (*Δpyhmgb2*; clones B3 and D1) were verified by PCR of genomic DNA (Fig.1B and data not shown) and Southern Blot using a *pyhmgb2* gene probe (Fig.1C). Disruption of the *pyhmgb2* locus resulted in a total loss of detectable *pyhmgb2* transcript expression by RT-PCR for the two clones (Fig 1D and data not shown) while the transcript of an unrelated gene [*pyada* (PY020760) Fig 1D, right panel] was not affected. Real time quantitative RT-PCR also confirmed that no residual expression of *pyhmgb2* gene could be detected.

The PyHMGB2 KO parasites are slightly attenuated during the asexual erythrocytic cycle.

We studied the effect of the disruption of the *pyhmgb2* locus on the asexual erythrocytic stage by examining growth of the parasite (Fig. 2A) as well as survival curves of mice infected by the WT or the *Δpyhmgb2* parasite strains (Fig. 2B). *Δpyhmgb2* parasite strains were able to proliferate normally and parasitemia was readably detectable after day 4. However, there was a delay in the onset of parasitemia in the *Δpyhmgb2* infected mice when compared to the WT parasite strain (Fig. 2A) and the mice infected by the *Δpyhmgb2* parasite strains survived longer, dying at days 8-9 post infection whereas mice infected with the WT parasite strain died 6-8 days after infection (Fig. 2B). The delay in the onset of parasitemia and the change in the kinetics of death of the mice were reproducible in experiments with both BALB/c and Swiss Webster mice (data not shown).

The Δpyhmgb2 parasites form gametocytes and ookinetes.

We examined whether the *Δpyhmgb2* parasites could complete the sexual cycle. The number of gametocytes on Giemsa stained blood smears was similar in mice infected with *Δpyhmgb2* parasite strains compared to the WT parasite after 2 days of infection (Table I). There were no significant differences in the level of mature gametocytes between the *Δpyhmgb2* parasite strains and the WT. The parasites were able to undergo gametocyte exflagellation (Table I), but *Δpyhmgb2* strains produced a decreased number of ookinetes when compared to the WT (Table I).

The Δpyhmgb2 parasites have dramatically impaired oocyst production.

We fed mosquitoes on mice infected with *Δpyhmgb2* and WT parasite strains bearing similar numbers of gametocytes and asexual stages. Eight days after feeding,

mosquito midguts were dissected and the number of oocysts scored using light microscopy. The number of infected mosquitoes for each strain was similar in each experiment (Table II). In three independent experiments, the mean number of oocysts per *Δpyhmgb2*-infected mosquito was approximately 10 % of the mean oocyst number seen in WT parasite infected mosquitoes (Table II). The oocysts produced by *Δpyhmgb2*-infected mosquitoes were able to complete the life cycle and produce viable sporozoites that were infectious to mice. The blood of the mice infected by those sporozoites was collected one week after infection. Using real time quantitative PCR we showed that these parasites do not express the *pyhmgb2* transcript and have the same genotype as the *Δpyhmgb2* parent (data not shown), indicating that no reversion of the disrupted allele had occurred.

Microarray comparison of Δpyhmgb2 and wildtype gene expression.

To examine the global expression profile of *Δpyhmgb2* parasites, we compared the transcriptome of *Δpyhmgb2* to the WT strain using a long oligonucleotide microarray designed to represent all the annotated genes of *P. yoelii*. These arrays have been previously validated to accurately reflect blood stage and liver stage *P. yoelii* gene expression (22,26). We harvested total RNA from a mixture of synchronized late erythrocytic stage parasites with similar numbers of gametocytes. Two independent clones of the *Δpyhmgb2* parasites were compared to the WT strain. Of the 6,428 annotated *P. yoelii* genes spotted on the array, only 32 genes showed differential expression in the KO (Table III). It is interesting to note that we found only downregulated genes in the *Δpyhmgb2* parasites. There was no detectable difference in expression of the transcript for *Pyhmb1* (PY05184).

The differential expression of 10 downregulated genes was independently confirmed by real time quantitative RT-PCR (Figure 3). We also confirmed, by real time quantitative RT-PCR, that the transcript coding for the PyHMGB1 (PY05184) protein was not differentially expressed, suggesting that compensation by the overexpression of another HMGB did not occur in the *Δpyhmgb2* parasites. Among control genes analyzed by qRT-PCR were those with ubiquitous expression [*pyada* (PY02076) or *pytubI* (PY01155); Fig. 3 and Supp. Fig 1] and other known gametocyte-specific genes whose expression was not altered by microarray analysis [Fig. 3 and Supp. Fig 1]. These were expressed at similar levels in WT and *Δpyhmgb2* parasites, confirming that the differences found by microarray profiling were not due to discrepancies in the number or maturity of asexual parasites and/or gametocytes present in the WT and *Δpyhmgb2* samples.

Down-regulated genes in the Δpyhmgb2 parasites are conserved and expressed at the gametocyte stage.

Among the genes down-regulated in the *Δpyhmgb2* parasite, we found *P. yoelii* homologues of the P25 and P28 ookinete genes (PY00522 and PY00523 respectively) and of *PfCCp2* (PY01580; also named *lap4* in *P. berghei*) that have a critical importance in oocyst development (27,28). Of the 32 genes, all but three were conserved among all *Plasmodium* species (Table III and Supp. Table I). Over 92 % of these genes are specifically expressed at the gametocyte stage or show enhanced expression at the gametocyte stage (Fig. 4). Transcripts of two *P. falciparum* homologues of down-regulated *P yoelii* genes (PY06201 and PY02893) are exclusively expressed at the asexual stage (Fig. 4).

We compared the steady state transcript levels in purified WT gametocytes and asexual erythrocytic forms for 10 of the genes down-regulated in the *Δpyhmgb2* by real-time quantitative RT-PCR (Fig. 5). As shown for its *P. falciparum* (29) and *P. berghei* homologues (4), the *pyhmgb2* transcript is over-expressed (8-fold) in gametocytes compared to asexual stages (Fig. 5). We confirmed that 8 of the down-regulated genes in the *Δpyhmgb2* parasites were specifically expressed or over expressed at the gametocyte stage in WT *P. yoelii* (Fig. 5). Analogous to its *P. falciparum* homologue, the

PY02893 transcript (adenosylhomocysteinase) is not overrepresented in gametocytes. Similarly, *pyada* transcript level was equivalent in gametocyte and asexual parasite extracts.

The peak of expression of the* Pfhmgb2 *transcript precedes or overlaps those of the down-regulated genes in the Δpyhmgb2 parasites.

We queried available expression profile data for gametocytogenesis of the *P. falciparum* 3D7 strain (3) for *pfhmgb2* and other orthologues of genes down-regulated in the *Δpyhmgb2* parasites (Supp. Figure 2 and Table III). The *pfhmgb2* transcript expression peaks between day 6 and day 8 of the gametocytogenesis of 3D7 strain, while the genes downregulated in the *Δpyhmgb2* parasites peak at day 8 (Supplementary Fig. 2 and Table III). Interestingly, the signal yielded by the oligonucleotides representing the two genes expressed exclusively at the asexual stage (Table III) does not follow this pattern (data not shown). These data are consistent with the hypothesized role of PyHMGB2 in the transcriptional regulation of the down-regulated genes.

Genes downregulated in the Δpyhmgb2 parasites encode proteins expressed at the ookinete stage.

Translational repression during *Plasmodium* sexual development is described as a major mechanism of gene regulation. We examined the proteomic data (4,30) available for the genes whose expression was down-regulated in the *Δpyhmgb2* parasites. Of the 18 genes transcripts down-regulated in the *Δpyhmgb2* parasites for which proteomic data is available, 16 (88%) had mRNA expressed at the gametocyte stage but only 5 had protein detectable in gametocytes (including 4 with both gametocyte and ookinete protein expression). Twelve of the 18 genes (67%; all with mRNA expressed in gametocytes stages) had gene products detected in only ookinetes or oocysts (Table III). Interestingly, more than 80% of the genes downregulated in the *Δpyhmgb2* parasites had their expression reduced by at least 2 fold in the ΔDOZI parasites (7) (Suppl. Table S1).

We performed an analysis of the expression of the PY00522 and PY00523 proteins, homologues of the *P. falciparum* Pfs25 and Pfs28 proteins. A similar number of *in vitro* cultured ookinetes from WT or *Δpyhmgb2* parasites was loaded on a polyacrylamide gel, separated by electrophoresis and subjected to Western Blot. As shown in figure 6A, the expression of PyADA (upper panel), was comparable in WT and KO, whereas the *Δpyhmgb2* parasites expressed approximately 3-4 fold less Pys25 and Pys28 protein as quantified by densitometry (Fig. 6B) in concordance with the trancriptomic data. An IFA performed on the *Δpyhmgb2* parasites in vitro cultured ookinetes did not reveal a subpopulation with expression of these two proteins at the WT level (data not shown).

Discussion

In this study, we investigated the role of the PyHMGB2 during the complete life cycle of the malaria parasite *P. yoelii*. HMGB1 and HMGB2 are highly conserved among *Plasmodium* species (16). The *P. falciparum* homologue of the PyHMGB2 protein is expressed by schizonts at the end of the erythrocytic asexual cycle and exhibits enhanced expression during gametocytogenesis (29). *P. yoelii* homologues follow the same pattern of expression as confirmed by real-time quantitative RT-PCR data (Fig.5).

Loss of expression of the *pyhmgb2* transcript during the erythrocytic asexual cycle in the mouse resulted in the delay of the onset of the parasitemia and time to death for the mice infected by the KO strains (Fig 2). Although *Δpyhmgb2* parasites are attenuated, PyHMGB2 is not essential during the asexual cycle of the parasite. The mild phenotype in asexual stages may be due to functional redundancy of PyHMGB2 with PyHMGB1 (16), but *Δpyhmgb2* parasites did not compensate with over-expression of the *pyhmgb1* transcript (Fig. 4).

Analysis of the *Δpyhmgb2* parasite transcriptome (Table III) revealed down-regulation of a subset of gametocyte transcripts. Two down-regulated genes, *P. yoelii* acid protease (PY06201) and adenosylhomocysteinase (PY02893) have *P. falciparum* orthologues exclusively expressed during the asexual cycle. The *P. berghei* homologue of the acid protease is expressed at the gametocyte stage indicating that this gene might be gametocyte-specific in rodent malarias (4). The adenosylhomocysteinase (PY02893) transcript expression profile was confirmed by real-time quantitative PCR (Fig. 5). *P. berghei* adenosylhomocysteinase protein is expressed in both asexual parasites and ookinetes ((4); www.plasmodb.org), indicating a potential role of this gene during both asexual and sexual development.

The majority of the genes that are differentially expressed in the KO have a homologue in all the *Plasmodium* species sequenced to date. In contrast, only 50 % of the genes induced at the gametocyte stage for *P. berghei* have a homologue in *P. falciparum* (4). Thus the genes whose expression is regulated by HMGB2 probably play conserved roles in all *Plasmodium* species.

The process of gametogenesis that is triggered in the mosquito after the blood meal is controlled by kinases that are able to rapidly induce a cascade of events in response to an external stimuli (31). Interestingly, none of the genes for these kinases is differentially regulated in the *Δpyhmgb2* parasites (Table III; Supp. Fig. 1).

The number and the maturity of the gametocytes were similar between *Δpyhmgb2* and the WT (Table I) suggesting that PyHMGB2 is not involved in the induction, commitment and establishment of the gametocytemia in the blood. Gametocyte exflagellation was also comparable in the *Δpyhmgb2* parasite when compared to the WT. Ookinete formation was significantly decreased in *Δpyhmgb2* and comparable to that found for a double knock-out of the P28 and P25 *P. berghei* genes (27,32). *In vivo*, we observed a drastic impairment of oocyst formation (Table II), although our microarray data indicate that PyHMGB2 regulates expression of genes transcribed in gametocytes.

We confirmed the gametocyte specific expression of 9 genes down-regulated in the *Δpyhmgb2* parasites, verifying concordance of the expression profiles in *P. falciparum*, *P. berghei* and *P. yoelii*. The *P. berghei* proteomic data suggest that many of these genes are translationally repressed until the ookinete stage (Table III) (4). However, due to limitations in sensitivity of proteomic technology, we cannot rule out that some genes down-regulated in the KO are expressed in other stages of the life cycle.

Translational repression seems to be widespread during the sexual stages of *Plasmodium* (7) and has been well characterized for Pbs25 and Pbs28, two proteins whose transcript levels are down-regulated in the KO (33). In accordance with the proteomics data, 80% of the genes downregulated in the *Δpyhmgb2* parasites (Supp. Table S1) have their expression at least partially controlled through the action of DOZI as shown by the microarray data collected for the *P. berghei* ΔDOZI parasites (7).

Three genes downregulated in the mutant parasites (Table III) have been disrupted in different *Plasmodium* species. The *Pbs21* (or *Pbs25*) and *Pbs28* genes, which encode surface proteins of ookinetes, have been shown to have redundant function as only a double KO exhibited a clear phenotype (27). The *P. berghei* strain with double KO of *Pbs21* and *Pbs28* has modest reduction of ookinete production and a drastic impairment of oocyst production in the mosquito (27). The ookinetes produced in the double KO are not able to cross the midgut epithelium, interact with the basal lamina and consequently do not produce oocysts (27). Similarly, *PfCcp2* (*P. falciparum*) and its orthologue *pblap4* (*P. berghei*) have been disrupted with a phenotype in the oocyst stage despite protein expression at the gametocyte stage (28,34). The observation that Pys25, Pys28 and PyCCP2 genes are downregulated in our mutant could be sufficient to explain the phenotype of the *Δpyhmgb2* parasite. Nevertheless, the other down-regulated genes could contribute to

ookinete and oocyst formation given their protein expression profile and conservation across *Plasmodium* species. For example 3 gametocyte specific articulins, a class of cytoskeletal proteins, are downregulated in the *Δpyhmgb2* parasites suggesting involvement of articulins in the maintenance of stage-specific cellular shapes (35).

The few oocysts generated by the *Δpyhmgb2* were able to produce a reduced number of infective sporozoites (data not shown). The *Pbs21* and *Pbs28* double KO parasites were also able to produce infective sporozoites (27). Therefore, PyHMGB2 appears to play a crucial role for the full expression of these genes but is not absolutely required.

Since the HMGB box family does not bind to DNA in a sequence-specific manner, PyHMGB2 is likely to be recruited to DNA by other factors or by a specific chromatin context (17). Interestingly, yeast two hybrid interaction data (36) show that HMGB2 is in the center of a broader network of proteins potentially involved in transcription regulation including 3 AP2 domain plant-like transcription factors (Supplementary Figure 3). AP2 proteins regulate the transcription of number of stress-induced pathways in plants (15). Genes for AP2 family members in *P. falciparum* are differentially expressed at specific developmental stages implicating them in transcriptional regulation of stage-specific gene expression (14). HMGB2 also interacts in yeast two hybrid with chromatin remodeling and modification enzymes like the acetyl-transferase GCN5 and a potential histone demethylase containing a Jumonji domain (36) (Supplementary Figure 3). PyHMGB2 may act cooperatively with AP2 sequence specific transcription factors and the chromatin modification machinery to control gene expression.

The sexual cycle of *Plasmodium* is a critical process required for transmission of malaria via the mosquito. In this study, we demonstrate that PyHMGB2 is not required for asexual growth but is involved in controlling genes important for oocyst development in the mosquito. Analysis of gene expression, proteomic and protein interaction data indicate that PyHMGB2 plays a pivotal role in controlling the transcriptional expression of a set of genes that are crucial for completion of the sexual cycle of malaria.

Acknowledgments.

The authors would like to thank Alida Coppi for sharing her expertise of the mosquito life cycle of *Plasmodium*. The authors would like to thank Sandra Gonzalez and Jean Nonon for their assistance with the rearing and infection of the mosquitoes. KK and LMT were supported by DOD PRMRP grant W81XWH-05-2-0025. PS was supported by NIH grant R01 AI056840. Design and construction of the *P. yoelii* microarray was supported by the NIH (to LWB). This work was supported by a Philippe Foundation fellowship to M.G.

Bibliography

1. Alano, P. (2007) *Mol Microbiol* **66**, 291-302
2. Le Roch, K. G., Johnson, J. R., Florens, L., Zhou, Y., Santrosyan, A., Grainger, M., Yan, S. F., Williamson, K. C., Holder, A. A., Carucci, D. J., Yates, J. R., 3rd, and Winzeler, E. A. (2004) *Genome Res* **14**, 2308-2318
3. Young, J. A., Fivelman, Q. L., Blair, P. L., de la Vega, P., Le Roch, K. G., Zhou, Y., Carucci, D. J., Baker, D. A., and Winzeler, E. A. (2005) *Mol Biochem Parasitol* **143**, 67-79
4. Hall, N., Karras, M., Raine, J. D., Carlton, J. M., Kooij, T. W., Berriman, M., Florens, L., Janssen, C. S., Pain, A., Christophides, G. K., James, K., Rutherford, K., Harris, B., Harris, D., Churcher, C., Quail, M. A., Ormond, D., Doggett, J., Trueman, H. E., Mendoza, J., Bidwell, S. L., Rajandream, M. A., Carucci, D. J., Yates, J. R., 3rd, Kafatos, F. C., Janse, C. J., Barrell, B., Turner, C. M., Waters, A. P., and Sinden, R. E. (2005) *Science* **307**, 82-86
5. Khan, S. M., Franke-Fayard, B., Mair, G. R., Lasonder, E., Janse, C. J., Mann, M., and Waters, A. P. (2005) *Cell* **121**, 675-687
6. Kumar, N., and Carter, R. (1985) *Mol Biochem Parasitol* **14**, 127-139
7. Mair, G. R., Braks, J. A., Garver, L. S., Wiegant, J. C., Hall, N., Dirks, R. W., Khan, S. M., Dimopoulos, G., Janse, C. J., and Waters, A. P. (2006) *Science* **313**, 667-669
8. Aravind, L., Iyer, L. M., Wellems, T. E., and Miller, L. H. (2003) *Cell* **115**, 771-785
9. Callebaut, I., Prat, K., Meurice, E., Mornon, J. P., and Tomavo, S. (2005) *BMC Genomics* **6**, 100
10. Gissot, M., Kelly, K. A., Ajioka, J. W., Greally, J. M., and Kim, K. (2007) *PLoS Pathog* **3**, e77
11. Voss, T. S., Kaestli, M., Vogel, D., Bopp, S., and Beck, H. P. (2003) *Mol Microbiol* **48**, 1593-1607
12. Dechering, K. J., Kaan, A. M., Mbacham, W., Wirth, D. F., Eling, W., Konings, R. N., and Stunnenberg, H. G. (1999) *Mol Cell Biol* **19**, 967-978
13. Gissot, M., Briquet, S., Refour, P., Boschet, C., and Vaquero, C. (2005) *J Mol Biol* **346**, 29-42
14. Balaji, S., Babu, M. M., Iyer, L. M., and Aravind, L. (2005) *Nucleic Acids Res* **33**, 3994-4006
15. Gutterson, N., and Reuber, T. L. (2004) *Curr Opin Plant Biol* **7**, 465-471
16. Briquet, S., Boschet, C., Gissot, M., Tissandie, E., Sevilla, E., Franetich, J. F., Thiery, I., Hamid, Z., Bourgouin, C., and Vaquero, C. (2006) *Eukaryot Cell* **5**, 672-682
17. Agresti, A., and Bianchi, M. E. (2003) *Curr Opin Genet Dev* **13**, 170-178
18. Arai, M., Billker, O., Morris, H. R., Panico, M., Delcroix, M., Dixon, D., Ley, S. V., and Sinden, R. E. (2001) *Mol Biochem Parasitol* **116**, 17-24
19. Carter, V., Nacer, A. M., Underhill, A., Sinden, R. E., and Hurd, H. (2007) *Int J Parasitol* **37**, 1221-1232
20. Jongco, A. M., Ting, L. M., Thathy, V., Mota, M. M., and Kim, K. (2006) *Mol Biochem Parasitol* **146**, 242-250
21. Mota, M. M., Thathy, V., Nussenzweig, R. S., and Nussenzweig, V. (2001) *Mol Biochem Parasitol* **113**, 271-278
22. Tarun, A. S., Peng, X., Dumpit, R. F., Ogata, Y., Silva-Rivera, H., Camargo, N., Daly, T. M., Bergman, L. W., and Kappe, S. H. (2008) *Proc Natl Acad Sci U S A*
23. Smyth, G. K. (2004) *Stat Appl Genet Mol Biol* **3**, Article3
24. Smyth, G. K. (2005) in *Bioinformatics and Computational Biology Solutions Using R and Bioconductor* (Gentleman, R., ed), pp. 397-420, Springer

25. Tsuboi, T., Cao, Y. M., Hitsumoto, Y., Yanagi, T., Kanbara, H., and Torii, M. (1997) *Infect Immun* **65**, 2260-2264
26. Shi, Q., Cernetich, A., Daly, T. M., Galvan, G., Vaidya, A. B., Bergman, L. W., and Burns, J. M., Jr. (2005) *Infect Immun* **73**, 6363-6371
27. Tomas, A. M., Margos, G., Dimopoulos, G., van Lin, L. H., de Koning-Ward, T. F., Sinha, R., Lupetti, P., Beetsma, A. L., Rodriguez, M. C., Karras, M., Hager, A., Mendoza, J., Butcher, G. A., Kafatos, F., Janse, C. J., Waters, A. P., and Sinden, R. E. (2001) *Embo J* **20**, 3975-3983
28. Raine, J. D., Ecker, A., Mendoza, J., Tewari, R., Stanway, R. R., and Sinden, R. E. (2007) *PLoS Pathog* **3**, e30
29. Le Roch, K. G., Zhou, Y., Blair, P. L., Grainger, M., Moch, J. K., Haynes, J. D., De La Vega, P., Holder, A. A., Batalov, S., Carucci, D. J., and Winzeler, E. A. (2003) *Science* **301**, 1503-1508
30. Florens, L., Washburn, M. P., Raine, J. D., Anthony, R. M., Grainger, M., Haynes, J. D., Moch, J. K., Muster, N., Sacci, J. B., Tabb, D. L., Witney, A. A., Wolters, D., Wu, Y., Gardner, M. J., Holder, A. A., Sinden, R. E., Yates, J. R., and Carucci, D. J. (2002) *Nature* **419**, 520-526
31. Billker, O., Dechamps, S., Tewari, R., Wenig, G., Franke-Fayard, B., and Brinkmann, V. (2004) *Cell* **117**, 503-514
32. Siden-Kiamos, I., Vlachou, D., Margos, G., Beetsma, A., Waters, A. P., Sinden, R. E., and Louis, C. (2000) *J Cell Sci* **113 Pt 19**, 3419-3426.
33. Paton, M. G., Barker, G. C., Matsuoka, H., Ramesar, J., Janse, C. J., Waters, A. P., and Sinden, R. E. (1993) *Mol Biochem Parasitol* **59**, 263-275
34. Pradel, G., Hayton, K., Aravind, L., Iyer, L. M., Abrahamsen, M. S., Bonawitz, A., Mejia, C., and Templeton, T. J. (2004) *J Exp Med* **199**, 1533-1544
35. Templeton, T. J., Iyer, L. M., Anantharaman, V., Enomoto, S., Abrahante, J. E., Subramanian, G. M., Hoffman, S. L., Abrahamsen, M. S., and Aravind, L. (2004) *Genome Res* **14**, 1686-1695
36. LaCount, D. J., Vignali, M., Chettier, R., Phansalkar, A., Bell, R., Hesselberth, J. R., Schoenfeld, L. W., Ota, I., Sahasrabudhe, S., Kurschner, C., Fields, S., and Hughes, R. E. (2005) *Nature* **438**, 103-107

Figure legends

Figure 1:

A: Schematic diagram of *pyhmgb2* gene disruption strategies. Sites of recombination are indicated in black. The *Hind*III restriction sites utilized in the Southern blot are indicated by the capital letter H. The position of the Southern probe is represented by an empty bar. Predicted size of the fragments is indicated under each locus. Arrows show the position of primers used in the diagnostic PCR.

B: Diagnostic PCR on genomic DNA extracted from *Δpyhmgb2* clone B3 and WT control parasite. Primer set A-T7 yielded a fragment of 1.2 kb size. Primer B-C amplified a 0.7kb fragment of the GFP gene. Amplification of the *pyada* gene (0.6 kb) is used as a PCR positive control (+). The data is representative of the two clones B3 and D1.

C: Southern Blot analysis of the *Hind*III digested gDNA for the WT, B3 and D1 clones. The sizes of the marker (M) are indicated on the right side of the figure. The thin arrow indicates the band expected for the WT locus. The bold arrows indicate the two bands expected for a disrupted locus.

D: RT-PCR analysis of the *pyada* and *pyhmgb2* transcript expression for a WT control (WT), a WT clone (B1) cloned at the same time as the KO clone (B3). Amplification of the *pyada* gene is used as a positive control (left panel). The RT-PCR shows that no expression of *pyhmgb2* (right panel) could be detected in the KO clone (B3). Data is representative of the two clones B3 and D1.

Figure 2:

A: Parasitemia (percentage of infected erythrocytes ± standard deviation) was monitored on Giemsa smears for the WT (straight line) and the *Δpyhmgb2* (dashed line) parasite lines during days 4 to 8 of the infection.

***: Statistically significant in a Two-way Anova Test (P<0.001).

B: Survival curves for mice infected by WT (straight line) and the *Δpyhmgb2* (dashed line) parasite lines. The average of three independent experiments (5 mice per group) with standard deviation is reported. Mice were monitored twice a day until all died. The difference between the survival curve is statistically significant as considered by the Log-rank (Mantel-Cox) Test (*p* value = 0.0023) or Gehan-Breslow-Wilcoxon Test (*p* value = 0.0039).

Figure 3: Real-time quantitative RT-PCR verifies down-regulation of genes differentially expressed between WT and *Δpyhmgb2* in microarray experiments.

Real-time quantitative RT-PCR data is represented by the black bars. The microarray data is represented by grey bars. The ratio of transcript expression in the WT parasites to transcript expression in KO is represented for the genes listed at the bottom of the graph. Differential expression was verified for 9 genes listed in Table III along with genes with ubiquitous expression (*Pypnp, PytubI, Pyhmgb1, Pyada*) or selected gametocyte specific genes whose expression was not affected in the KO (*PytubII, Pywarp, Pys36,* PY06600, *pys48/45,* PY00415, *Pynima*). A thick black line delimits the ratio for which genes are downregulated in the KO when compared to the WT.

Figure 4: Distribution of the of the expression peaks for the *P. falciparum* homologues of the downregulated genes in the *Δpyhmgb2* parasites. Expression data was available on PlasmoDB (www.plasmodb.org) and from (2) for 27 downregulated genes among the 29 genes conserved in at least *P. falciparum* and another *Plasmodium* species. 25 of the 27 genes (92%) show peak expression at the gametocyte stage (black bar). Genes expressed during the asexual stage exclusively or at the asexual and gametocyte stages (9 out of 27; 33 %) are represented by a white bar. 17 of the 27 genes (63%) show expression only at the gametocyte stage (dark gray bar). Genes expressed in only the asexual stages (2 out of 27; 7%) are represented by a light gray bar.

Figure 5: Genes downregulated in the KO are expressed specifically at the gametocyte stage of WT *P. yoelii* parasites.

Quantification of the relative level of expression in gametocytes and asexual stages of WT *P. yoelii* parasites for 10 genes downregulated in the KO was performed using real-time quantitative RT-PCR. The normalized ratio of the measured transcript expression in purified gametocyte over asexual parasites in the WT parasites is represented for the genes listed at the bottom of the graph. A thick black line marks the ratio for which genes are over-expressed in gametocytes when compared to their expression in asexual parasites.

Figure 6: Pys28 and Pys25 proteins are downregulated in KO ookinetes.

A: Western Blot analysis of PyADA expression in WT and KO ookinetes (upper panel). Pys28 and Pys25 (lower panel) were detected in WT and KO cultured ookinetes.

B: Densitometry quantification of the expression of Pys28 and Pys25 proteins. Values for WT and KO protein levels were normalized using the PyADA loading control. Comparisons between WT and KO are presented in arbitrary units. WT values are represented with black bars. KO values are represented by grey bars.

Table I: Δ*pyhmgb2* parasites form *in vitro* ookinetes less efficiently.

		Gametocytemia (%) [a]	Exflagellation [b]	Ookinete formation (*in vitro*)[c] (%)
Experiment 1	WT	0.36	57 +/- 12	100
	KO	0.25	63 +/- 14	51.6[d]
Experiment 2	WT	0.56	43 +/- 16	100
	KO	0.49	39 +/- 12	63.2[d]

[a]: Percentage of gametocytes per 100 RBC. Two mice were infected with each strain.
[b]: Exflagellation: The number of exflagellation centers per 10000 RBC divided by the number of male gametocytes per 10000 RBC multiplied by 100.
[c]: Ookinetes were produced by *in vitro* culture as described in the materials and methods. Efficiency of ookinete formation is expressed as the percentage of the WT control.
[d]: Statistically significant in a non-paired t-test (p value < 0.05)

Table II: Δ*pyhmg2 in vivo* oocyst production is impaired.

		Mean number of oocysts[a]	Oocyst prevalence[b]
Experiment 1	WT	65.5 ± 24	94.1
	KO	7.8 ± 4.9 *	81.6
Experiment 2	WT	92.1 ± 38	100.0
	KO	15.7 ± 7.8 *	82.0
Experiment 3	WT	64 ± 19	48.0
	KO	4.3 ± 3.2 *	48.0

[a]: The mean number of oocysts per infected mosquito ± SD.

[b]:Percentage of mosquito midguts containing oocysts. 50 midguts were dissected for each experiment.

*: Statistically significant in a non-paired t-test (p value < 0.0001)

Table III: Microarray analysis of Δ*Pyhmgb2 clones* reveals down-regulation of conserved sexual stage genes.

	Annotation	**FC**[a]	**Transcriptomics *P. falciparum*[b]**	**Transcriptomics *P. berghei*[c]**	**Proteomics *P. berghei*[d]**	**Ortholog *P. falciparum*[e]**
PY07077	high mobility group protein 2	6.16	Gametocyte and Schizonts	Gametocyte		MAL8P1.72
PY03130	STOP repeat protein	4.22*	Gametocyte	Gametocyte	Ookinete	PFI0460w
PY00522	ookinete surface antigen-like protein Pys25	4.16*	Gametocyte	Gametocyte	Ookinete and Oocysts	PF10_0303
PY00523	ookinete surface antigen-like protein Pys28	4.13*	Gametocyte		Ookinete and Oocysts	PF10_0302
PY00860	hypothetical protein	3.04	Gametocyte and Schizonts	Gametocyte	Ookinete	PF14_0522
PY04557	hypothetical protein	2.61	Gametocyte	Gametocyte	Ookinete	PF13_0220
PY05340	hypothetical protein	2.39	Gametocyte and Schizonts		Ookinete	PF08_0073
PY00380	hypothetical protein	2.38	Gametocyte		Ookinete	PFL2320w
PY01580	LCCL domain-containing protein CCP2	2.33	Gametocyte and Schizonts	Gametocyte	Gametocyte and Ookinete	PF14_0532
PY00220	SAC3/GANP/Nin1/mts3/eIF-3 p25 domain protein	2.07				PFF0125c
PY01624	PfFNPA, a protein in the gametocyte-specific PfCCp family	2.06	Gametocyte	Gametocyte	Gametocyte and Ookinete	PF14_0491
PY03088	Pfs77 protein-related ; articulin	1.97*	Gametocyte	Gametocyte	Ookinete	PF13_0226
PY06201	Acid protease	1.91	Merozoite and Sporozoite		Gametocyte	PFL1660c
PY02871	hypothetical protein	1.87	Gametocyte and Schizonts	Gametocyte	Ookinete	PF11_0422
PY01183	Zinc finger domain protein	1.86	Gametocyte	Gametocyte		PF13_0314
PY07861	Hypothetical protein	1.85				
PY04502	articulin	1.84	Gametocyte and Schizonts	Gametocyte	Gametocyte and Ookinete	PF08_0033
PY02014	hypothetical protein	1.78				

PY01757	4 tandem kelch domains followed by a BTB/POZ domain	1.77		Gametocyte		
PY02893	adenosylhomocysteinase	1.73*	Schizonts		Asexual and Ookinete	PFE1050w
PY01887	hypothetical protein	1.71	Gametocyte	Gametocyte		PF08_0024
PY02308	hypothetical protein	1.68	Gametocyte and Schizonts	Gametocyte	Ookinete	PFD0520c
PY01032	hypothetical protein	1.66	Gametocyte		Gametocyte	PF08_0023
PY06780	hypothetical protein	1.65	Gametocyte			PFB0177c
PY00469	Eukaryotic aspartyl protease Plasmepsin	1.64	Gametocyte			PF10_0329
PY01137	articulin	1.63	Gametocyte	Gametocyte	Ookinete	PFL1030w
PY07430	calcium/calmodulin-stimulated cyclic nucleotide phosphodiesterase, putative	1.63	Gametocyte			PF14_0672
PY04297	Plasmodium falciparum CPW-WPC domain	1.62*	Gametocyte			PF13_0168
PY02878	hypothetical protein	1.61	Gametocyte and Schizonts		Ookinete	MAL7P1.74
PY01150	epsilon-adaptin, putative-related	1.6				PFI0200c
PY00977	exonnuclease, putative	1.55*	Gametocyte			MAL13P1.311
PY01299	ortholog of AMY-1	1.34*	Gametocyte			PF07_0060

[a]: FC= fold change calculated as normalized signal intensity of the wild type *P. yoelii* YM divided by normalized signal intensity of the KO (two clones). Data are from 2 biological replicates hybridized to the oligonucleotide array as discussed in the materials and methods (8 hybridization signals per gene for wild type). Data from the two KO clones were combined (16 hybridization signals per gene). All genes that showed significant change were downregulated in the KO. Downregulation of genes with an asterisk was verified by quantitative RT-PCR (Figure 3).

[b]: as reported by Le Roch *et al.* (2) (data publicly available at www.plasmodb.org).

[c]: upregulated in gametocytes as reported by Hall *et al.*(4)

[d]: as reported by Hall *et al.*(4) (data publicly available at www.plasmodb.org).

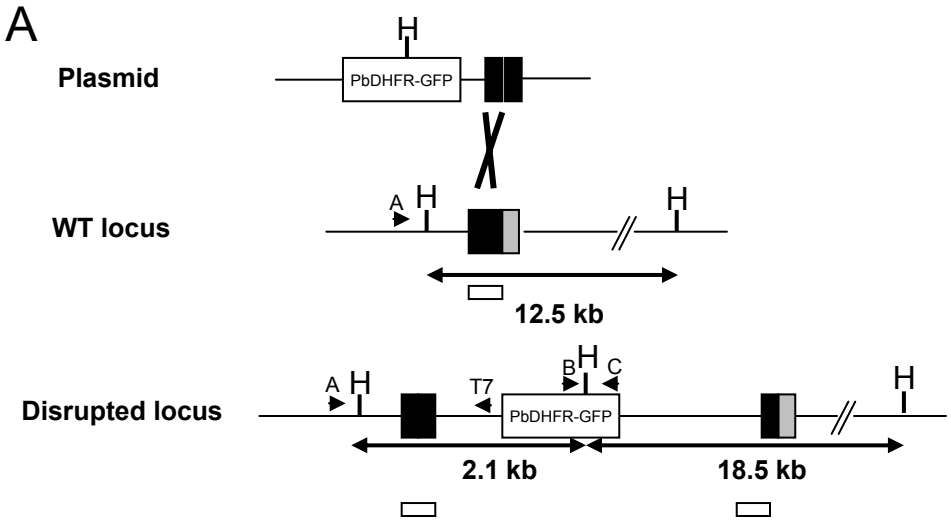
A
Plasmid
H
PbDHFR-GFP
WT locus
A
H
H
12.5 kb
Disrupted locus
A
H
T7
B
H
C
PbDHFR-GFP
H
2.1 kb
18.5 kb

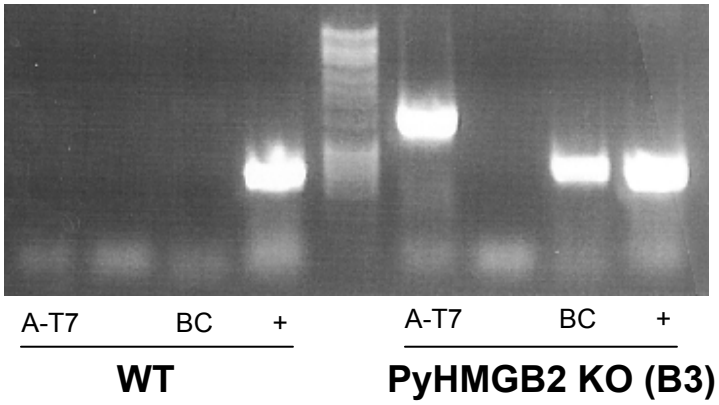
B
A-T7
BC
+
A-T7
BC
+
WT
PyHMGB2 KO (B3)

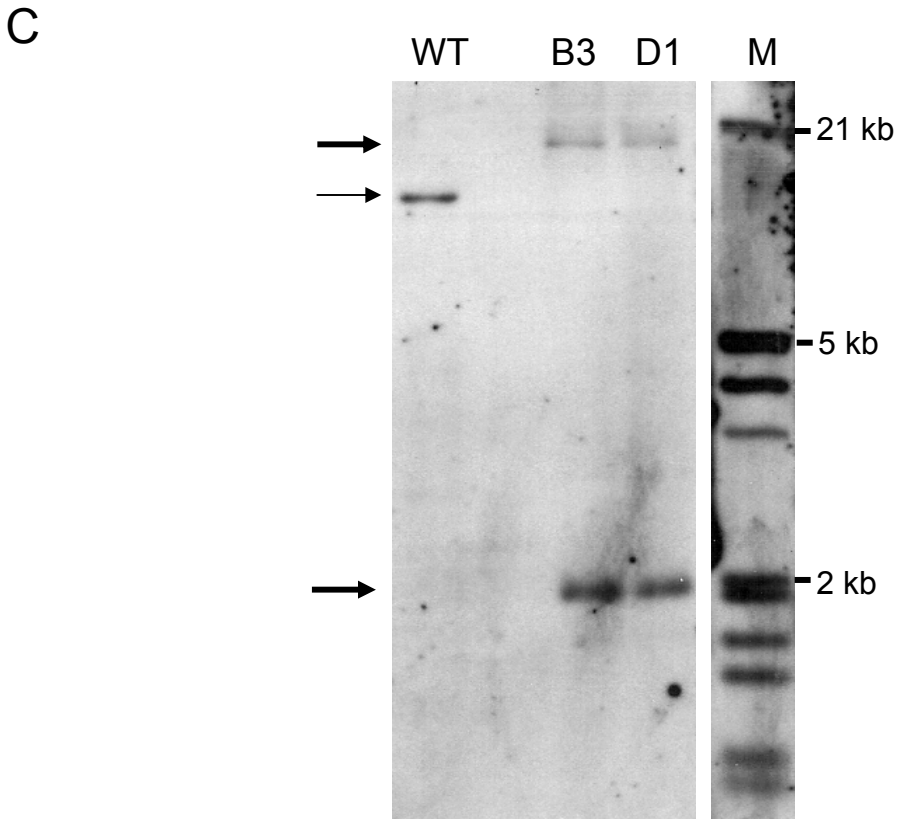
C
WT
B3
D1
M
21 kb
5 kb
2 kb

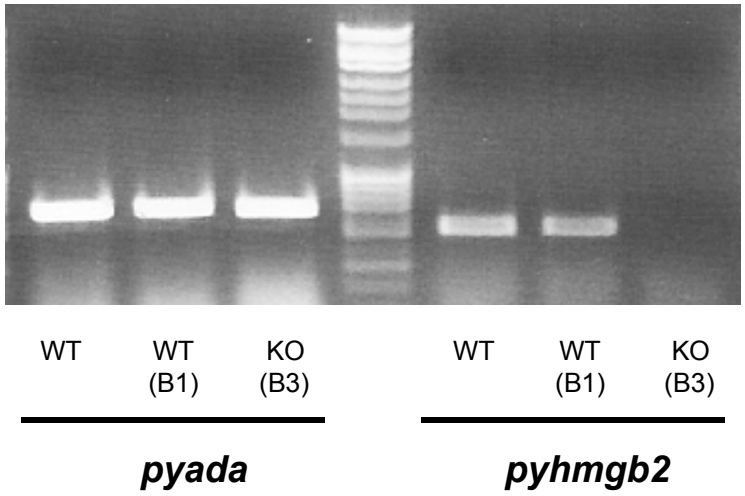
D
WT
WT (B1)
KO (B3)
WT
WT (B1)
KO (B3)
pyada
pyhmgb2

2

A

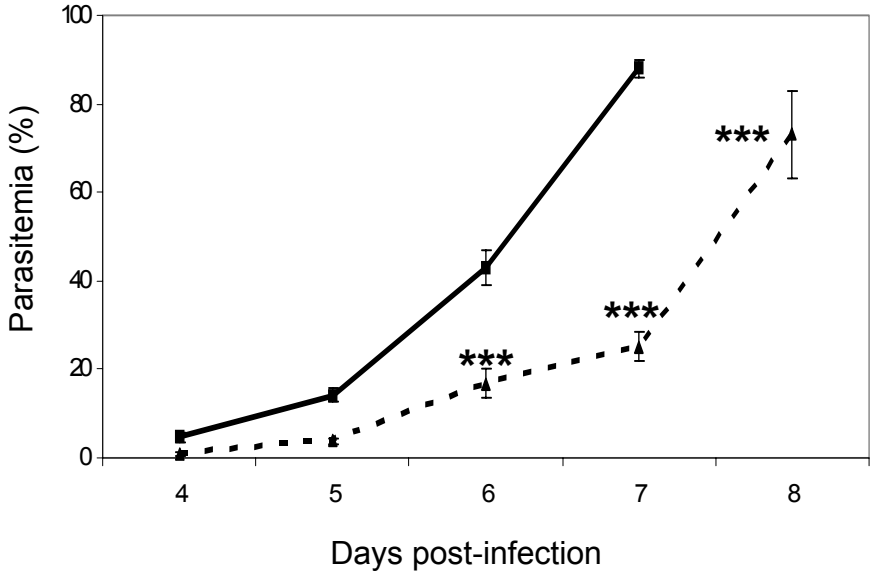
Parasitemia (%)
100
80
60
40
20
0
4
5
6
7
8
***
***
Days post-infection

B

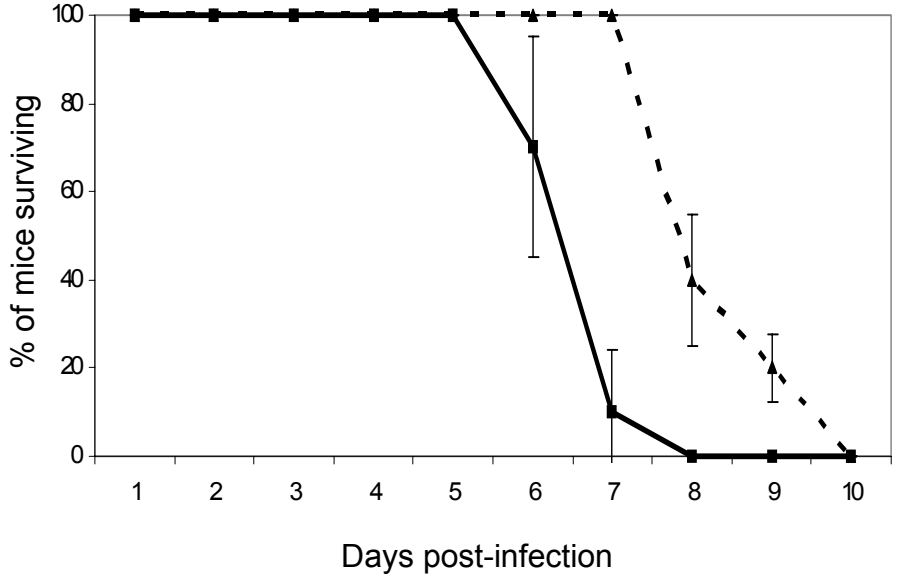
% of mice surviving
100
80
60
40
20
0
1
2
3
4
5
6
7
8
9
10
Days post-infection

3

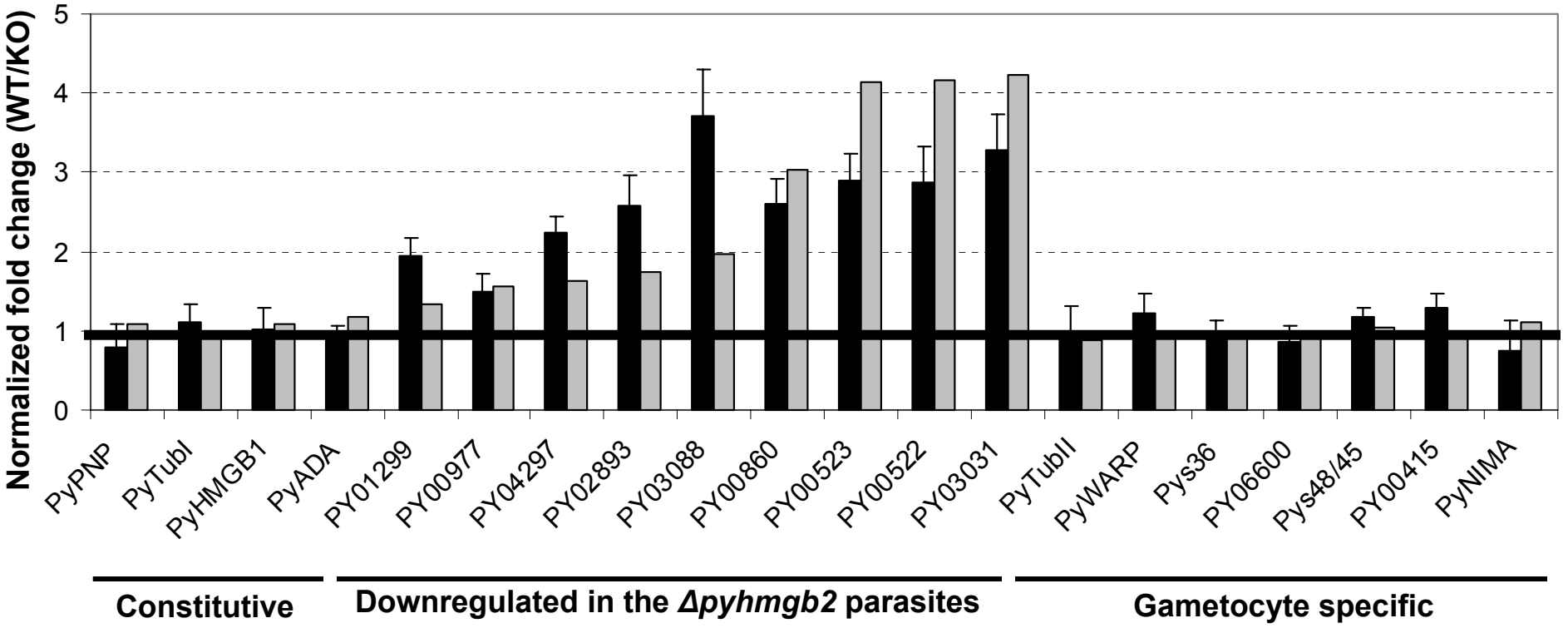
Normalized fold change (WT/KO)
5
4
3
2
1
0
PyPNP
PyTubI
PyHMGB1
PyADA
PY01299
PY00977
PY04297
PY02893
PY03088
PY00860
PY00523
PY00522
PY03031
PyTubII
PyWARP
Pys36
PY06600
Pys48/45
PY00415
PyNIMA
Constitutive
Downregulated in the Δpyhmgb2 parasites
Gametocyte specific

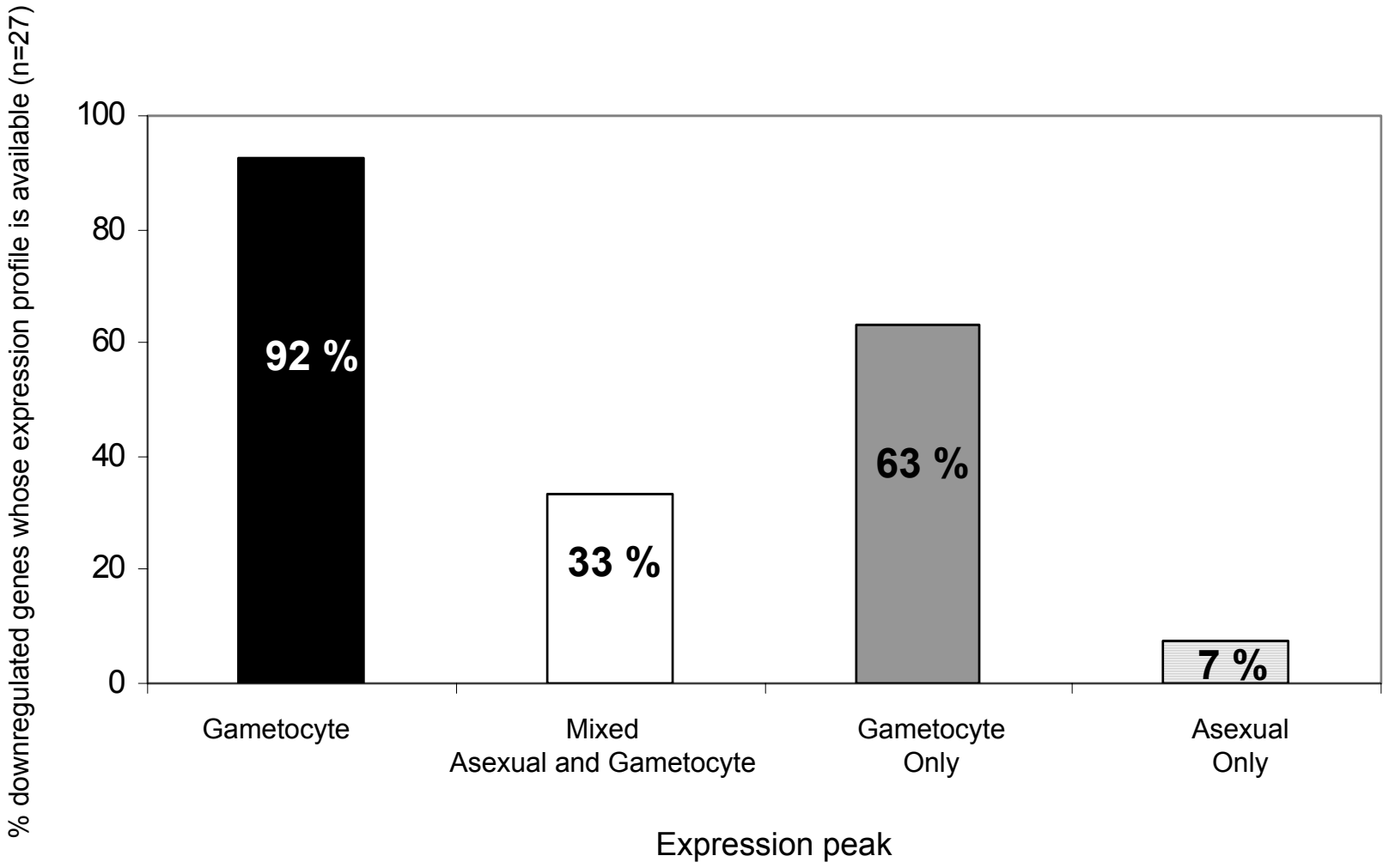
% downregulated genes whose expression profile is available (n=27)
100
80
60
40
20
0
92 %
33 %
63 %
7 %
Gametocyte
Mixed
Asexual and Gametocyte
Gametocyte
Only
Asexual
Only
Expression peak

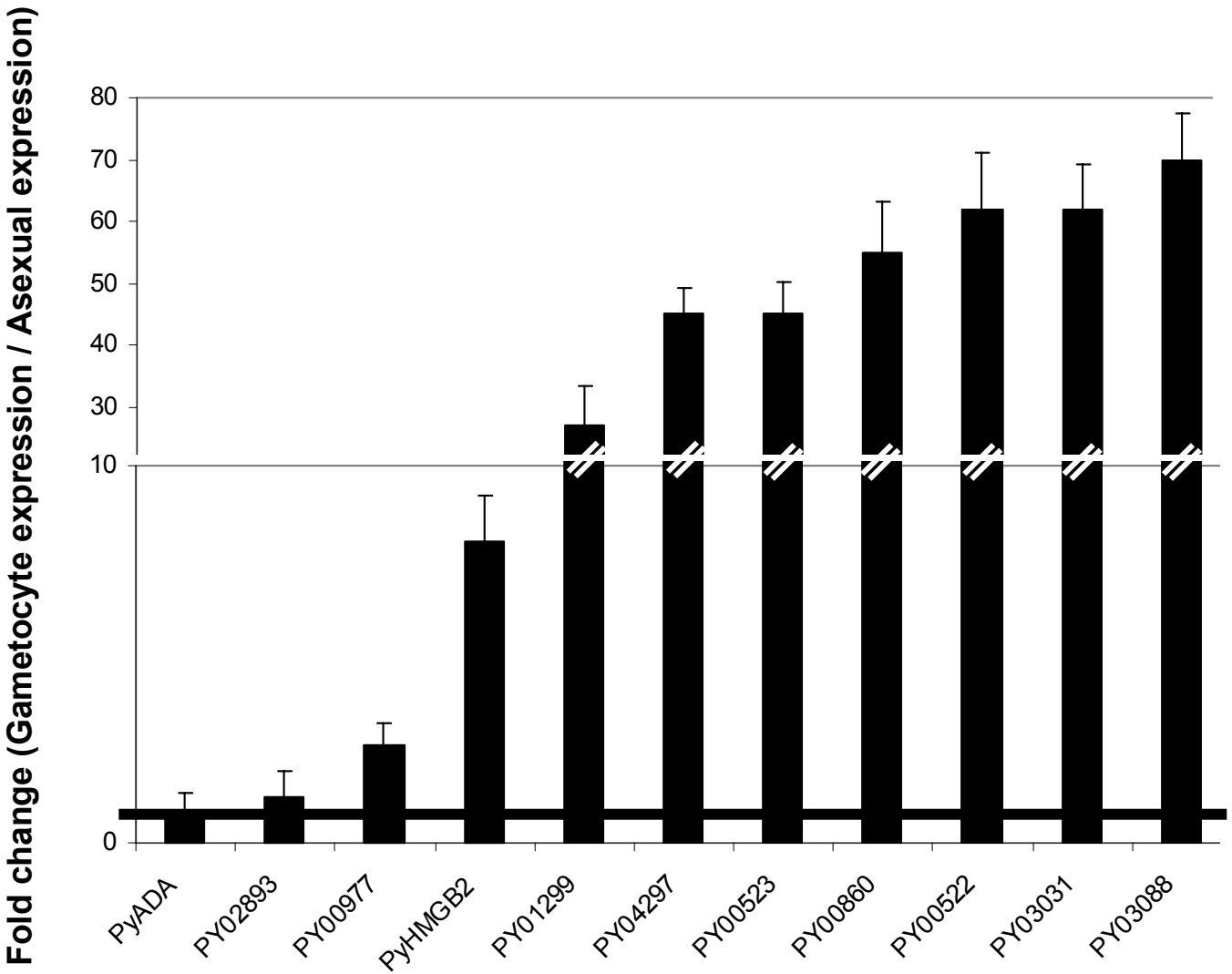
Fold change (Gametocyte expression / Asexual expression)
80
70
60
50
40
30
10
0
PyADA
PY02893
PY00977
PyHMGB2
PY01299
PY04297
PY00523
PY00860
PY00522
PY03031
PY03088

6A

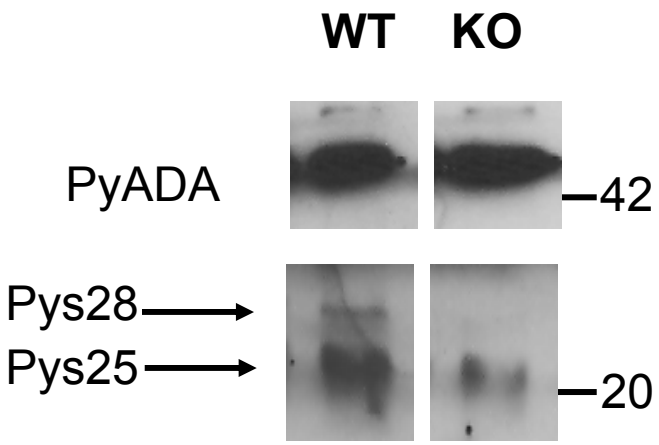
WT
KO
PyADA
42
Pys28
Pys25
20

6B

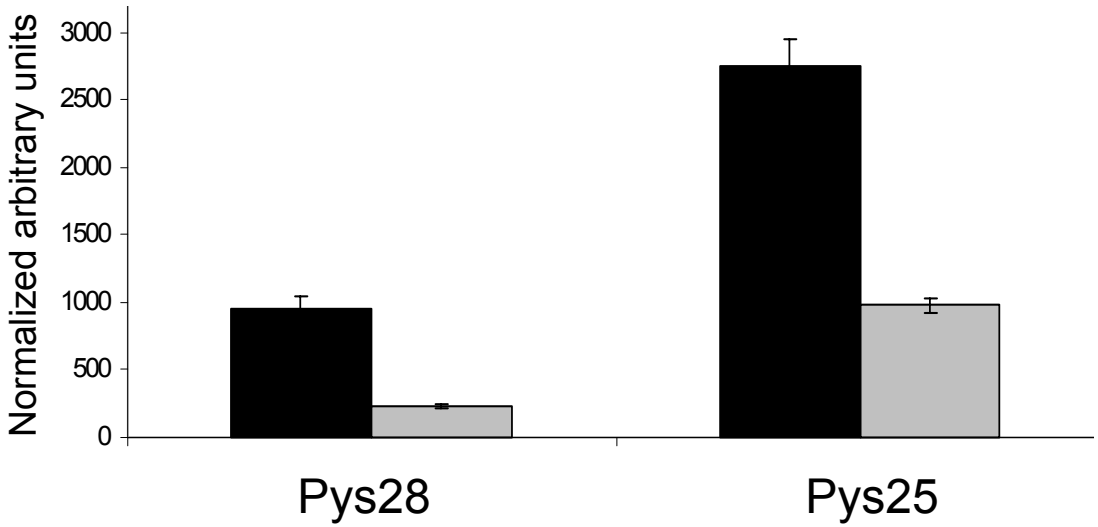
Normalized arbitrary units
3000
2500
2000
1500
1000
500
0
Pys28
Pys25